Ocean biogeochemistry with ECCO and Darwin

Dimitris Menemenlis
Jet Propulsion Laboratory
California Institute of Technology

ECCO Summer School 2019
May 19–31, 2019
Friday Harbor Laboratories
University of Washington
Friday Harbor, WA

Sensitivity of CO_2 Sea Air Flux

The unrealistically large CO_2 flux during ENSO present in the filtered solution (left) due to anomalous vertical advection is corrected in the smoothed estimate (right) consistent with observations.

Filtered Estimate

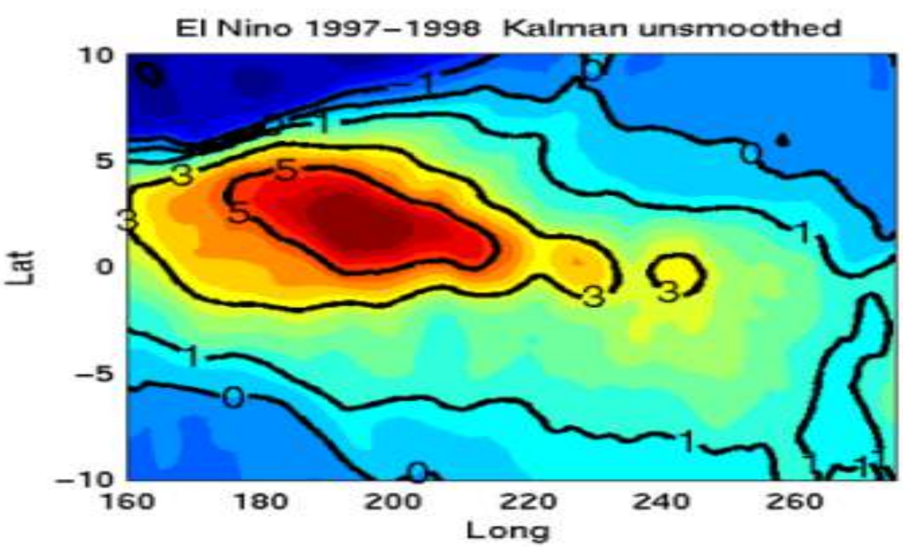

Smoothed Estimate

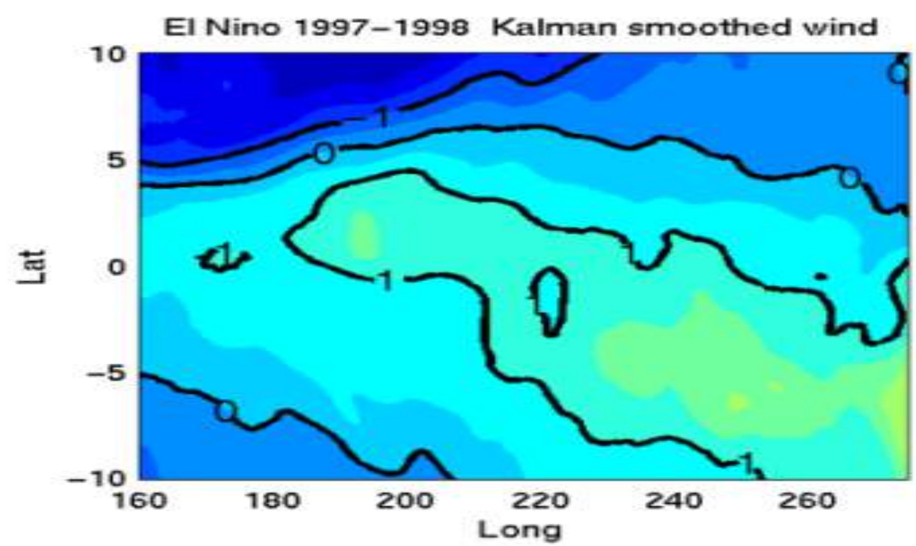

(G.McKinley, 20

Ocean Carbon-cycle Model Intercomparison Project 3 (OCMIP-3) (Mikaloff Fletcher et al. 2006, 2007; Gruber et al. 2009)

Table 1. Evaluation of Model Skill Based on Comparisons Between CFC-11 Model Simulations and the GLODAP Gridded CFC Data Set[a]

	Correlation	Normalized Std. Dev.[b]	Model Skill[c]	Inverse Anthropogenic CO_2 Uptake, Pg C yr^{-1}	Forward Anthropogenic CO_2 Uptake, Pg C yr^{-1}
BERN	0.89	1.04	0.81	2.05	N.A.
ECCO	0.96	0.89	0.91	2.01	N.A.
MIT	0.91	1.00	0.85	2.22	N.A.
NCAR	0.95	0.98	0.91	2.18	2.36
PRINCE-LL	0.90	1.18	0.80	1.85	1.90
PRINCE-HH	0.93	1.05	0.87	2.33	2.43
PRINCE-LHS	0.93	1.04	0.86	1.99	2.04
PRINCE-2	0.93	1.03	0.87	2.17	2.24
PRINCE-2a	0.91	1.05	0.85	2.25	2.35
UL	0.87	1.0	0.77	2.81	2.95
Mean	0.92	1.02	0.85	2.18	2.32

CFC-11 experiment using ECCO-v0 has highest correlation, lowest standard error, and highest model skill relative to observations!

Dream of implementing time-evolving, data-constrained biogeochemistry on top of CS510, circa 2005 …

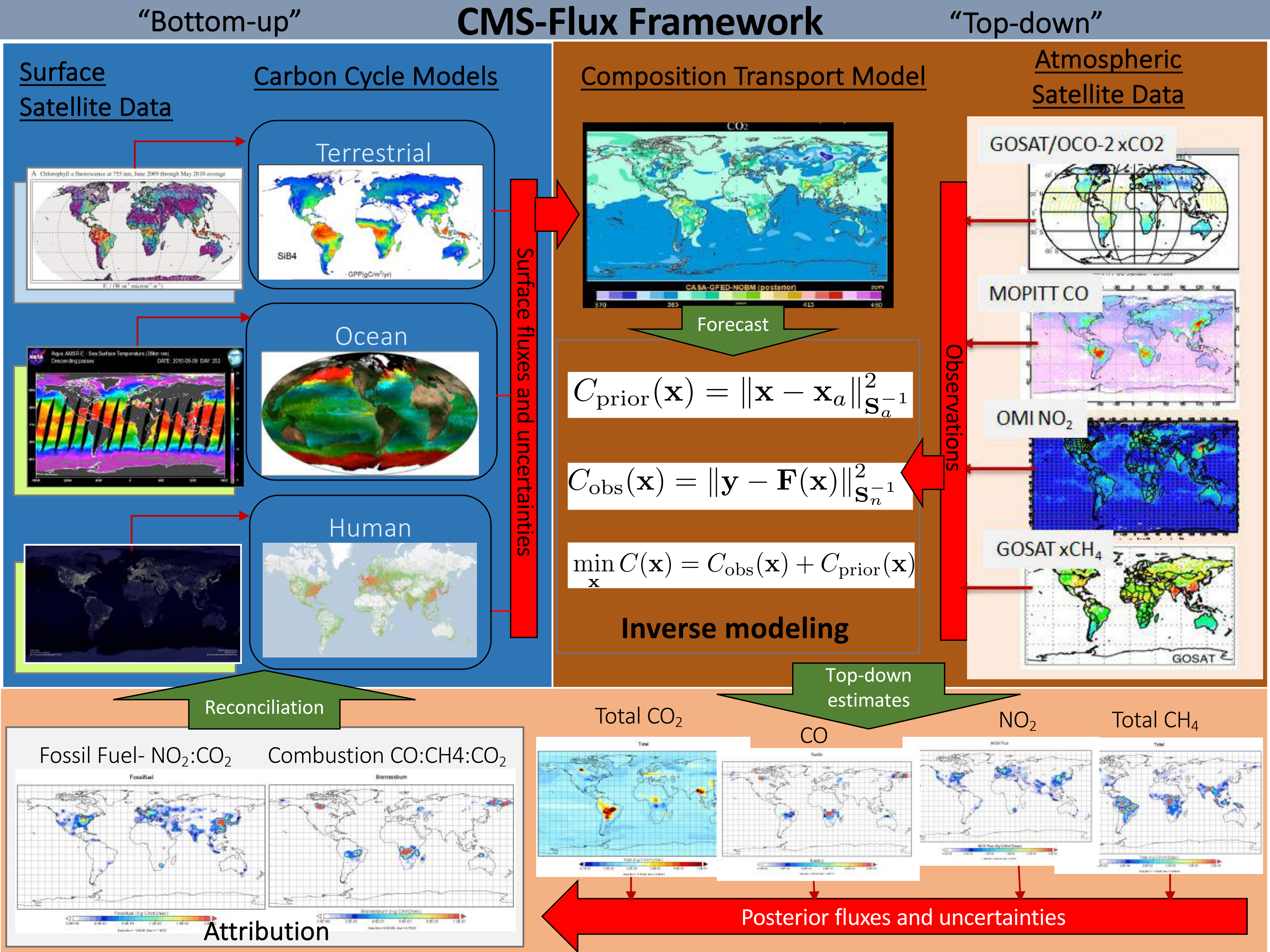
"Bottom-up"
CMS-Flux Framework
"Top-down"
Surface Satellite Data
Carbon Cycle Models
Composition Transport Model
Atmospheric Satellite Data
Terrestrial
SiB4
Ocean
Human
Surface fluxes and uncertainties
CO2
CASA-GFED-NOBM (posterior)
Forecast
$C_{\text{prior}}(\mathbf{x}) = \|\mathbf{x} - \mathbf{x}_a\|^2_{\mathbf{S}_a^{-1}}$
$C_{\text{obs}}(\mathbf{x}) = \|\mathbf{y} - \mathbf{F}(\mathbf{x})\|^2_{\mathbf{S}_n^{-1}}$
$\min_{\mathbf{x}} C(\mathbf{x}) = C_{\text{obs}}(\mathbf{x}) + C_{\text{prior}}(\mathbf{x})$
Inverse modeling
Observations
GOSAT/OCO-2 xCO2
MOPITT CO
OMI NO_2
GOSAT xCH_4
GOSAT
Reconciliation
Top-down estimates
Fossil Fuel- NO_2:CO_2
Combustion CO:CH4:CO_2
Fossilfuel
Biomassburn
Attribution
Total CO_2
CO
NO_2
Total CH_4
Posterior fluxes and uncertainties

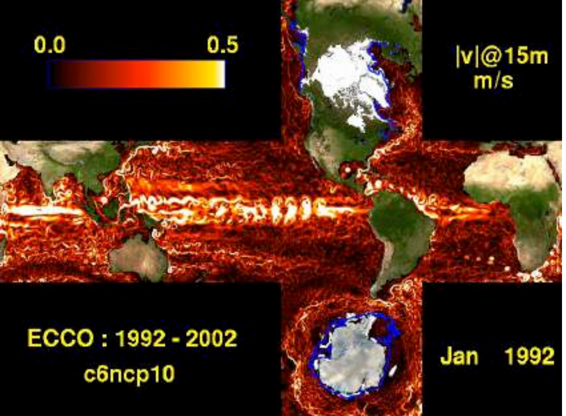

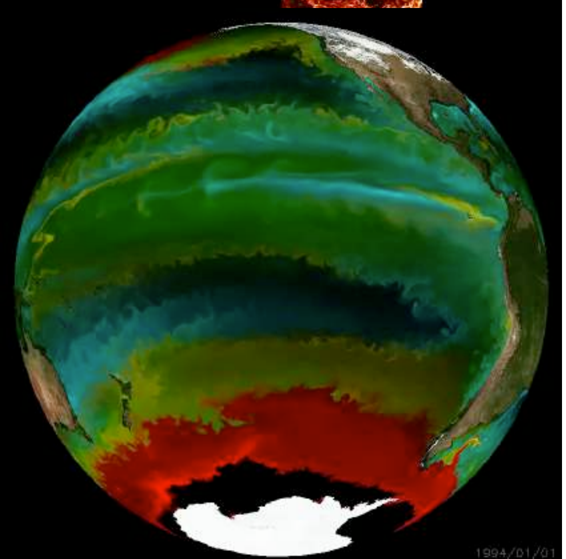

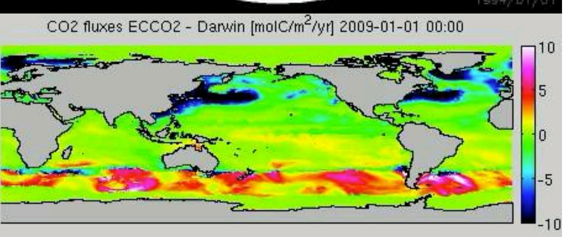

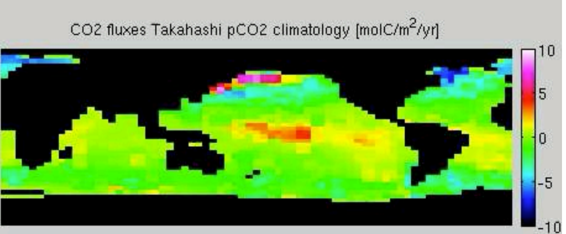

Sales pitch to NASA Carbon Monitoring System (CMS) Pilot Study circa ~2010 …

ECCO2: an eddying ocean and sea ice data synthesis

- Eddying, full-depth ocean and sea ice state estimates based on constraining a numerical model with satellite and in situ data using the adjoint method (Menemenlis et al., 2008).

Darwin: a self-organizing marine ecosystem model

- The Darwin Project is an initiative to advance development and application of novel models of marine microbial communities, identifying the relationships of individuals and communities to their environment, connecting cellular-scale processes to global microbial community structure (Dutkiewicz et al., 2009).

ECCO2/Darwin ocean surface carbon flux estimates

- Together, ECCO2 and Darwin provide a time-evolving physical and biological environment for carbon biogeochemistry.

Global, Eddying, Ocean Ecology and Biogeochemistry Model

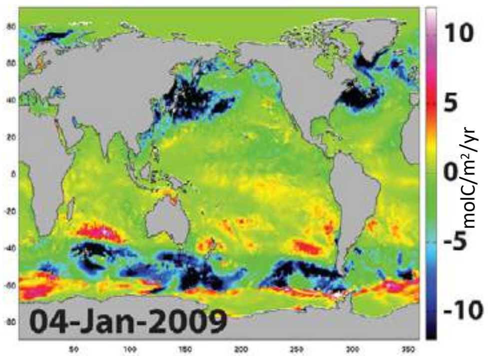

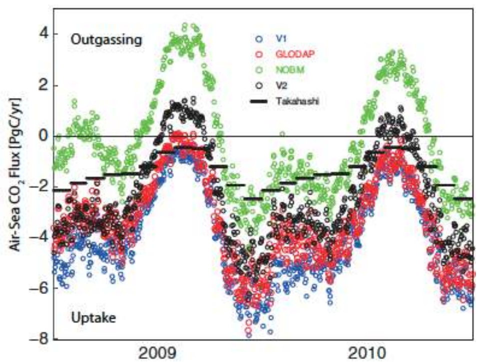

Problem: Global ocean biogeochemistry models suitable for Carbon Monitoring System (CMS) Flux studies require high spatial and temporal resolution to capture fine scale structure of carbon sources and sinks. The problem addressed here is initialization/adjustment of such a model to minimize drift and distance from observations.

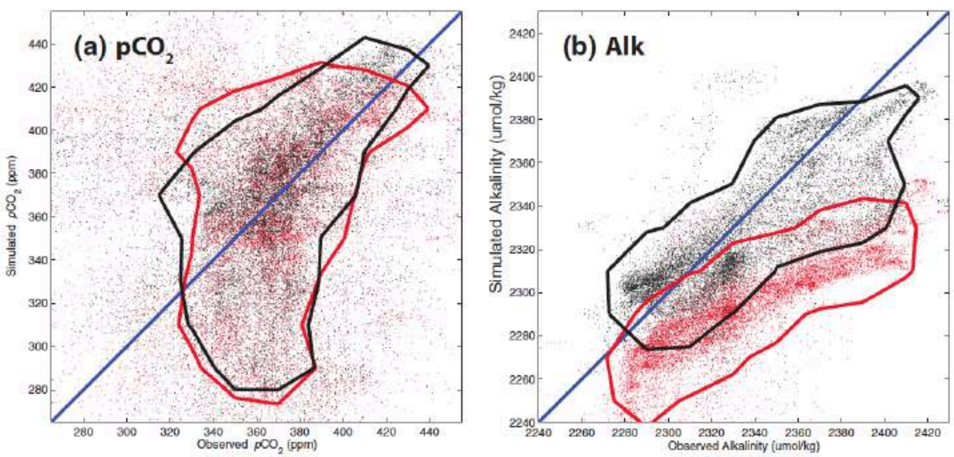

Finding: The trajectory of a global, eddying ocean biogeochemistry model can be adjusted to simultaneously reduce drift and distance from observations using a Green's function approach.

Significance: The adjusted simulation is a first step towards a more accurate representation of ocean carbon cycle at high spatial and temporal resolution, suitable for studies of global air-sea-land exchanges of carbon and ocean acidification.

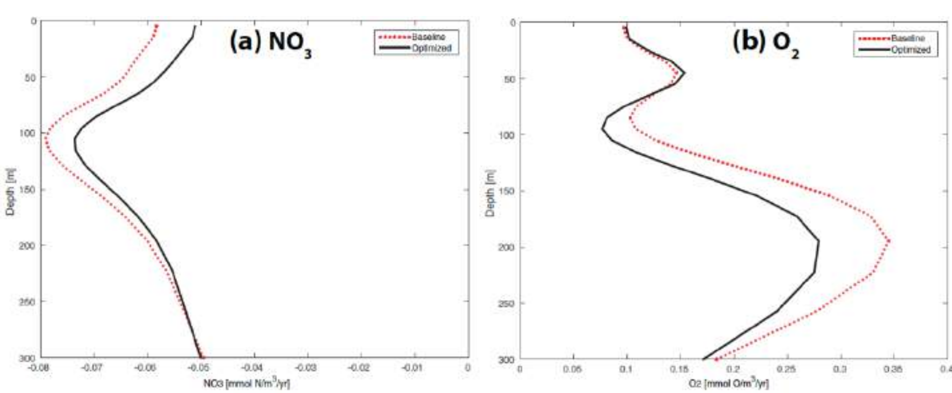

Top left: Example sea-air CO_2 gas flux showing impact of ocean upwelling and synoptic atmospheric variability (negative values indicate ocean uptake).

Top right: Globally integrated sea–air CO_2 fluxes for 2009 and 2010 for four different model realizations (baseline is blue circles, two model Green's functions in red and green circles, and optimized in black circles), vs Takahashi Atlas (black lines).

Middle: Scatter plot of observed (x-axis) and simulated (y-axis) pCO2 (left) and Alkalinity (right) for baseline (red) and optimized (black) simulations.

Bottom: Global volume-weighted trend vs. depth plots for nitrate (left) and oxygen (right), for the baseline (red) and optimized (black) simulations.

H. Brix, et al., *Ocean Model.* 2015: Using Green's Functions to initialize and adjust a global, eddying ocean biogeochemistry general circulation model.

ENSO Impact on Ocean Carbon Uptake

The El Nino/La Nina in 2010-2011 was the largest Central Pacific ENSO event in the satellite record. These led to a record-breaking tropical North Atlantic anomaly that in turned caused the once-in-a-century Amazonian droughts.

What was the impact of the El Nino on ocean carbon?

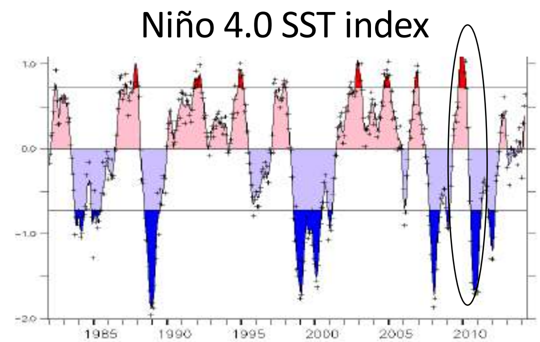

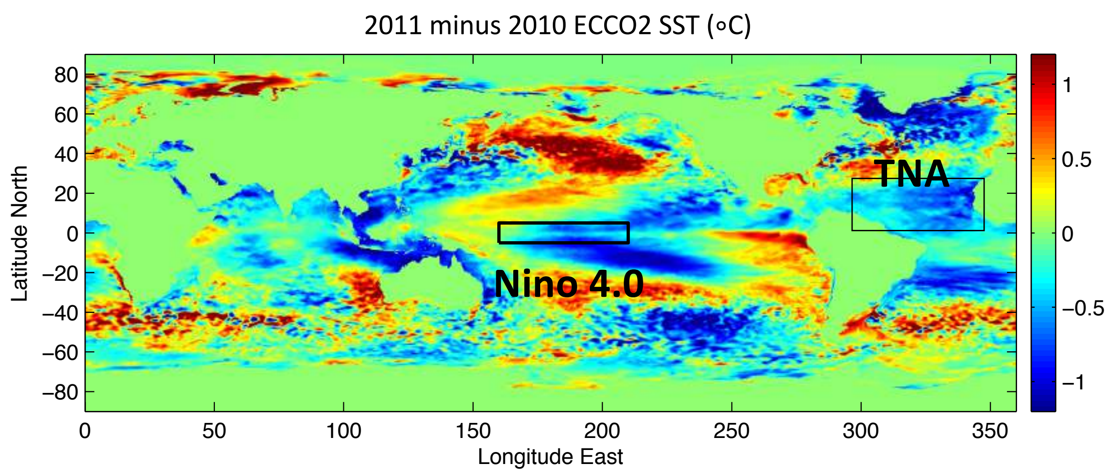

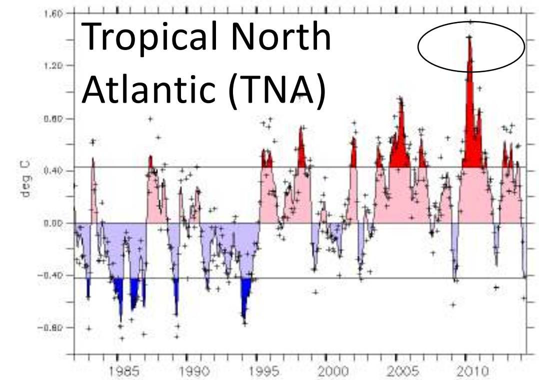

2011 experienced cooler SSTs in the Eq. Pacific & N. Atlantic in association with a strong La Niña.

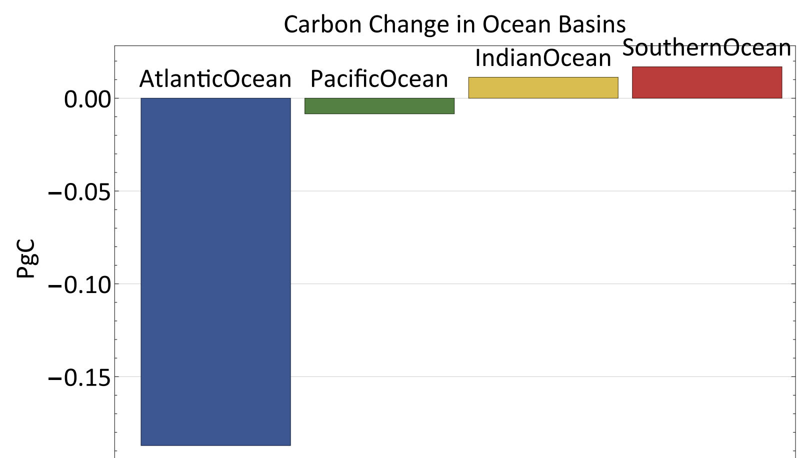

The Atlantic Ocean flux (-0.18 PgC) accounts for more than half of the total ocean carbon change (-0.33 PgC) and is equivalent to the drought response in Brazilian flux (Bowman et al. 2017)

... but there were indications of trouble in ECCO-Darwin paradise ☹

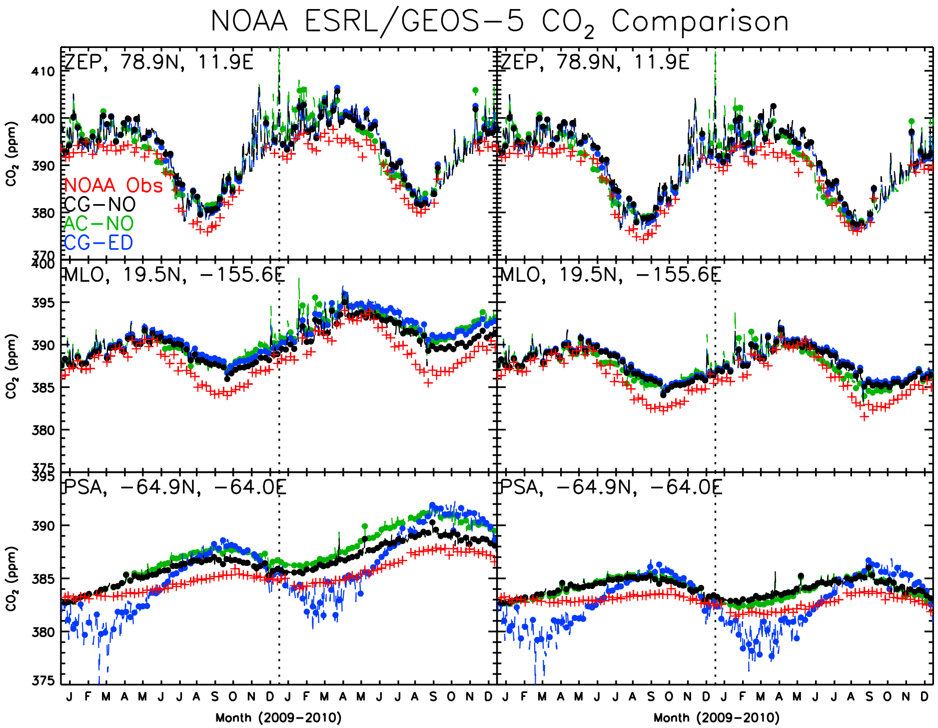

Ott et al., 2015

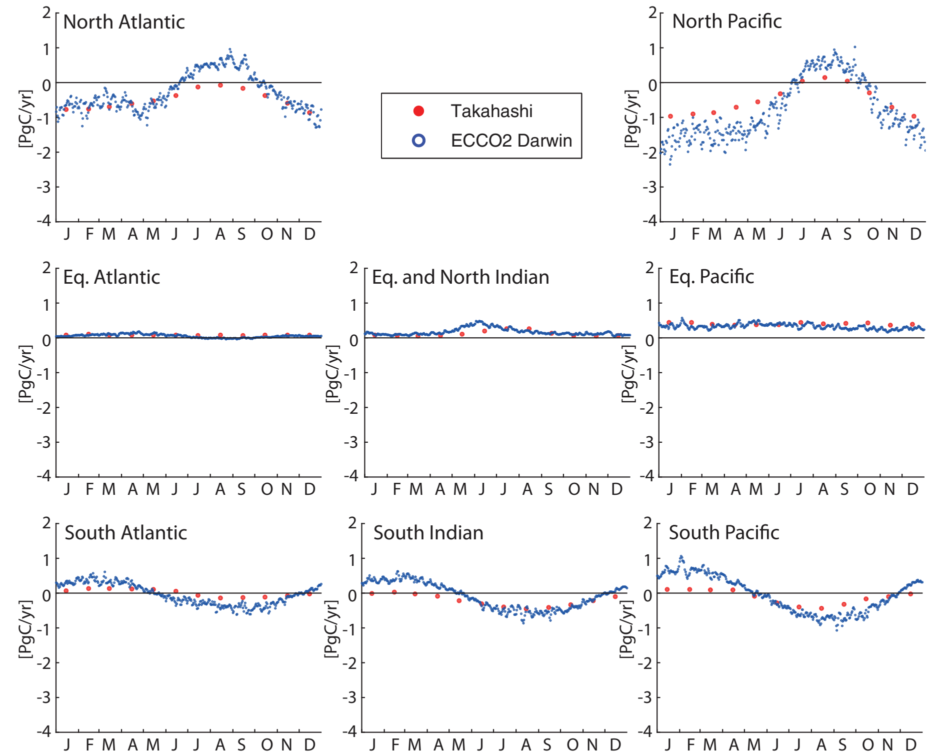

Brix et al. 2015 (fineprint)

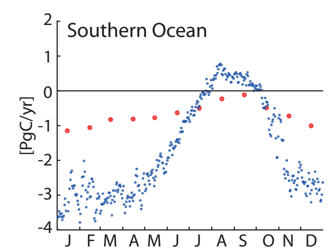

tions and prior model parameter estimates. After some experimentation, we used the following data constraints ($\mathbf{y}^o$ in Eqs. (4)–(6)): (1) surface pCO_2 data for 2009 and 2010 from the "Global Surface pCO_2 (LDEO) Database" at the Carbon Dioxide Information Analysis Center (Takahashi et al., 2011) as described in Section 5, (2) a global mean air–sea CO_2 flux of 2.4 PgC yr^{-1} for 2010 from the Global Carbon Project (2011), and (3) the Takahashi et al. (2009) Atlas for the seasonal cycle of pCO_2 after removing area-weighted monthly means from the original values. The standard errors (the square root of the

As we constrained our model to achieve a "target" global carbon uptake of about 2.4–2.5 PgC yr^{-1}, it needs to compensate for the too strong carbon uptake in the Southern Ocean by weaker uptake or intensified outgassing in other regions. The model achieves this compensation mainly in the mid-latitude summers of both hemispheres (compare Fig. 9). Additional Green's Functions sensitivity

Enter Dustin to the rescue!

Rest of presentation shows results from D. Carroll et al. (submitted).

Quixotic quest to build the best ocean carbon model in the world!

ECCO-Darwin v4

Physics: ECCO LLC 270, Jan 1992–May 2018

Biology: 5 Phytoplankton and 2 Zooplankton types

Biogeochemical ICs:

- GLODAP V2 climatology (Lauvset *et al.* 2016)
- ECCO-Darwin v2 (Brix *et al.* 2015)

Forcing:

- Atmospheric pCO_2 forcing (NOAA MBL)
- Monthly climatological iron dust forcing (Mahowald *et al.* 2009)

Observational Constraints (n = 4038777):

- SOCAT V5 surface fCO_2 (Bakker *et al.* 2016)
- GLODAP V2 profiles (Olsen *et al.* 2017)
- SOCCOM BGC-Argo profiles (Riser *et al.* 2018)
- UW Argo O_2 profiles (Drucker and Riser, 2016)

Optimization:

- 13 biogeochemical Green's Functions

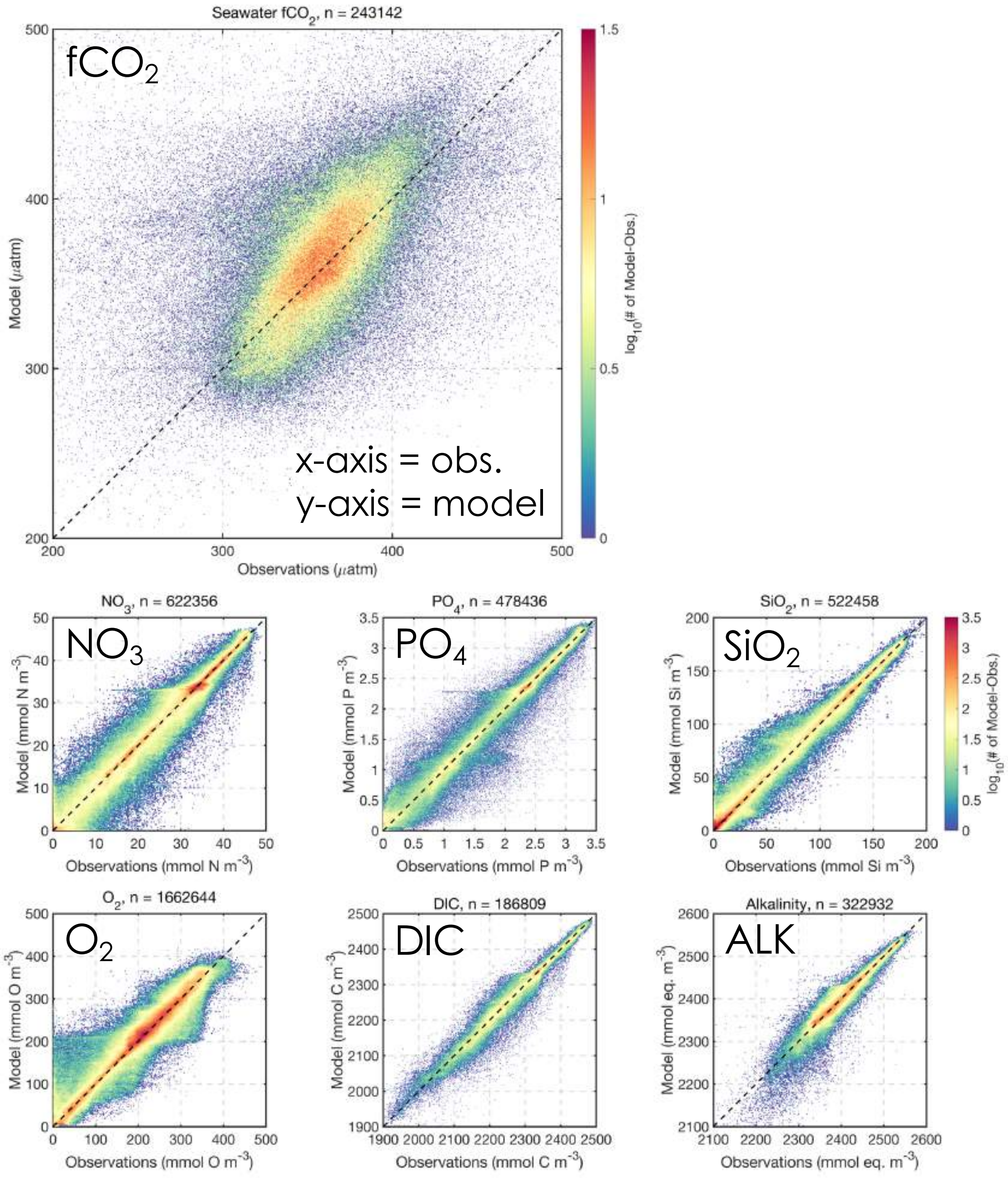

Table S1.

All simulations used in the ECCO-Darwin v4 Green's Function's optimization.

Orange, blue, and green rows show the first-guess baseline, baseline, and final optimized simulation, respectively.

Perturbation Pair (simulation, baseline)	Perturbation Experiment	Piston Velocity Formulation	Biogeochemical Initial Conditions	Parameter (initial, perturbed, optimized)	Linear Combination Coefficient	Cost per Observation
1, N/A	Linear piston velocity	Linear	Brix et al. (2015) V2	N/A	0.08802	0.35067
2, 1	Iron dust solubility reduced by 20%	Linear	Brix et al. (2015) V2	1, 0.8, 0.92734	0.36328	0.35023
3, 1	Initial conditions set to January 1996	Linear	Simulation #2 January 1996	N/A	-0.17383	0.35527
4, 1	Initial conditions set to January 1998	Linear	Simulation #2 January 1998	N/A	-0.27747	0.35926
5, 12	Quadratic piston velocity	Quadratic	Simulation #2 January 1996	N/A	0.011553	0.35564
6, 12	DIC and alkalinity initial conditions increased by 150 mmol C m^{-3} and 150 mmol eq. m^{-3}, respectively	Quadratic	Simulation #2 January 1996 with adjusted DIC/alkalinity	N/A	-0.0059469	0.24431
7, 12	DIC and alkalinity initial conditions from GLODAPv2 climatology	Quadratic	Simulation #2 January 1996 with GLODAPv2 DIC/alkalinity	N/A	-0.21831	0.13334
8, 12	NO_3, PO_4, SiO_2, O_2, DIC, and alkalinity initial conditions from GLODAPv2 climatology	Quadratic	Simulation #2 January 1996 with GLODAPv2 NO_3, PO_4, SiO_2, O_2, DIC, and alkalinity	N/A	0.044263	0.11712
9, 12	Iron scavenging rate increased by 500%	Quadratic	Simulation #2 January 1996 with GLODAPv2 NO_3, PO_4, SiO_2, O_2, DIC, and alkalinity	3, 15, 9.3208	0.52673	0.11510
10, 12	Particulate inorganic carbon to particulate organic carbon ratio increased by 20%	Quadratic	Simulation #2 January 1996 with GLODAPv2 NO_3, PO_4, SiO_2, O_2, DIC, and alkalinity	0.04, 0.048, 0.041914	0.23927	0.11689
11, 12	Small phytoplankton growth rate increased by 10%	Quadratic	Simulation #2 January 1996 with GLODAPv2 NO_3, PO_4, SiO_2, O_2, DIC, and alkalinity	0.7, 0.77, 0.69176	-0.11774	0.11949
12, N/A	Large phytoplankton growth rate increased by 10%	Quadratic	Simulation #2 January 1996 with GLODAPv2 NO_3, PO_4, SiO_2, O_2, DIC, and alkalinity	0.4, 0.44, N/A	0.56397	0.11547
13, 12	Diatom palatability increased by 0.1	Quadratic	Simulation #2 January 1996 with GLODAPv2 NO_3, PO_4, SiO_2, O_2, DIC, and alkalinity	0.85, 0.95, 0.84562	-0.043787	0.11901
14, N/A	Optimized Solution	Quadratic	Linear combination of initial conditions shown above	Optimized values shown above	N/A	0.11148

93% cost reduction from trial and error, not Green's Functions optimization.

ECCO-Darwin v4 CO_2 Flux

Red = CO_2 outgassing
Blue = CO_2 uptake

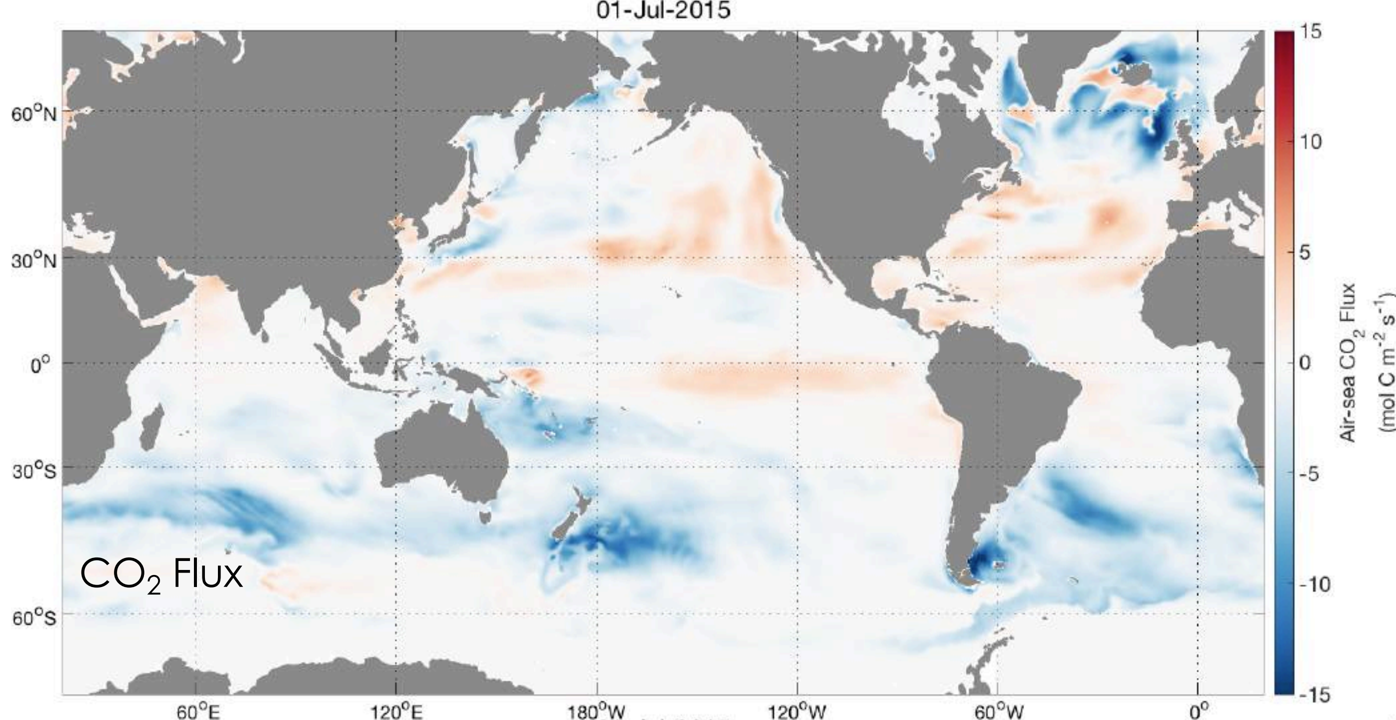

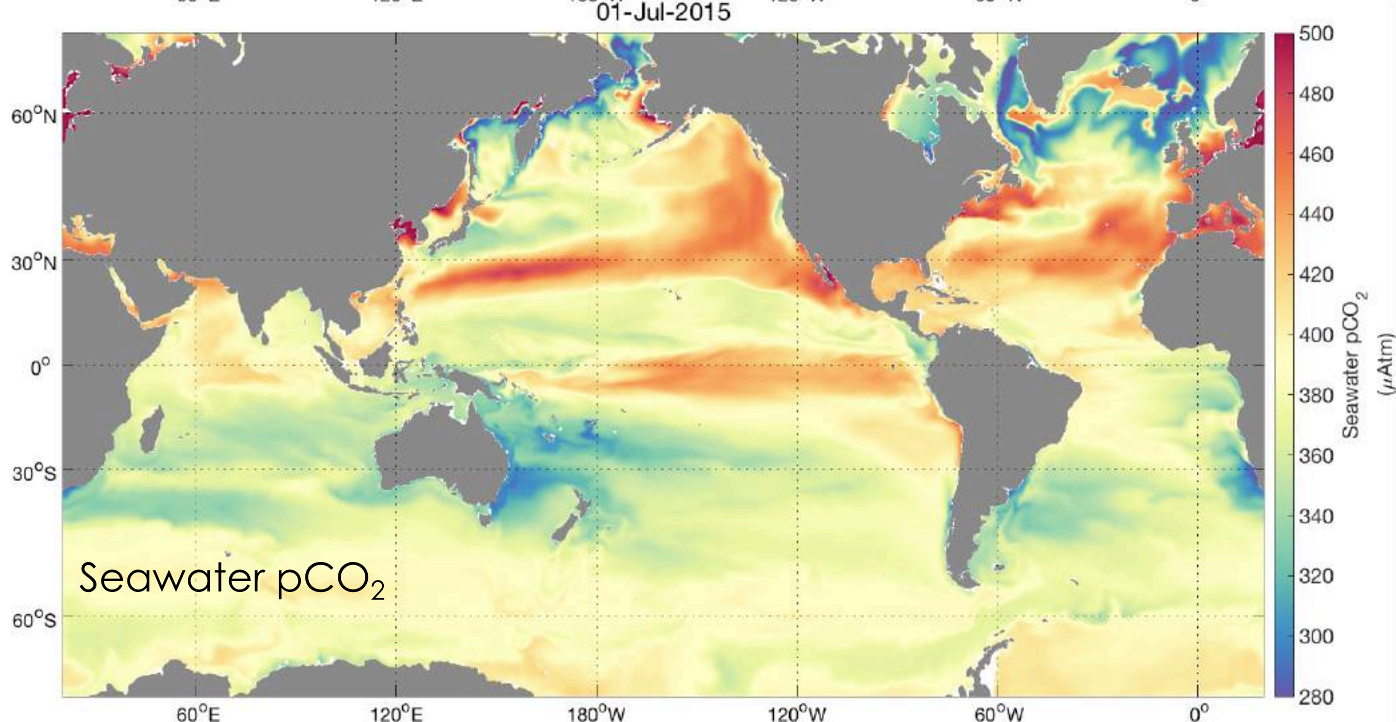

Mean global air-sea CO_2 fluxes for:
(a) Takahashi 2009,
(b) Rödenbeck 2013
(c) Landschützer 2013
(d) ECCO-Darwin v4.

Positive values represent outgassing (red); negative values show uptake (blue).

Tak09 is referenced to year 2000;

Röd13, Land13, and ED are time-averaged from January 1995 to December 2017.

Regions north of 80N in Tak09, Röd13, and Land13 are excluded due to data sparsity.

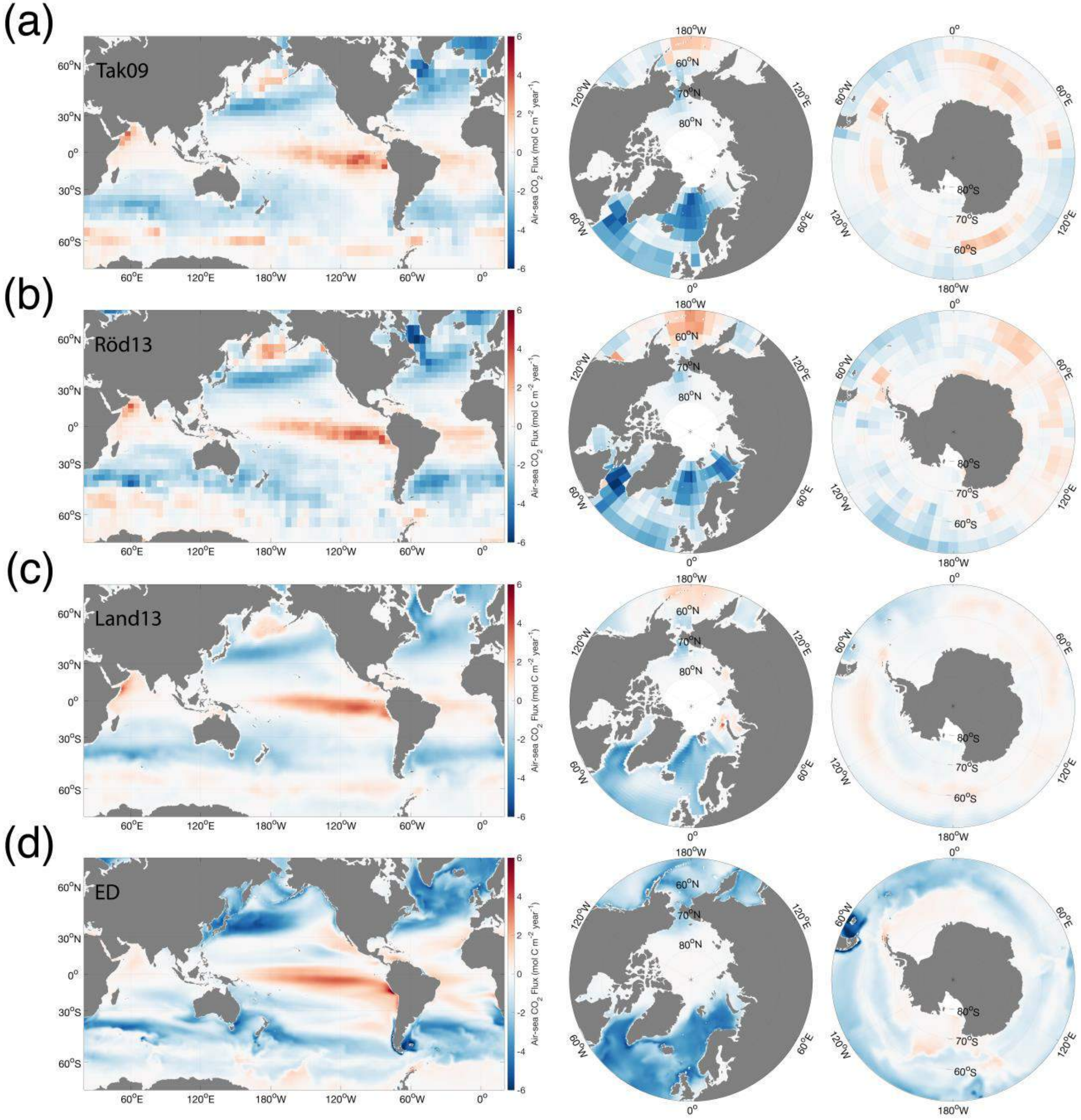

Mean surface ocean pCO_2 fluxes for:
(a) Takahashi 2009,
(b) Rödenbeck 2013
(c) Landschützer 2013
(d) ECCO-Darwin v4.

Tak09 is referenced to year 2000;

Röd13, Land13, and ED are time-averaged from January 1995 to December 2017.

Regions north of 80N in Tak09, Röd13, and Land13 are excluded due to data sparsity.

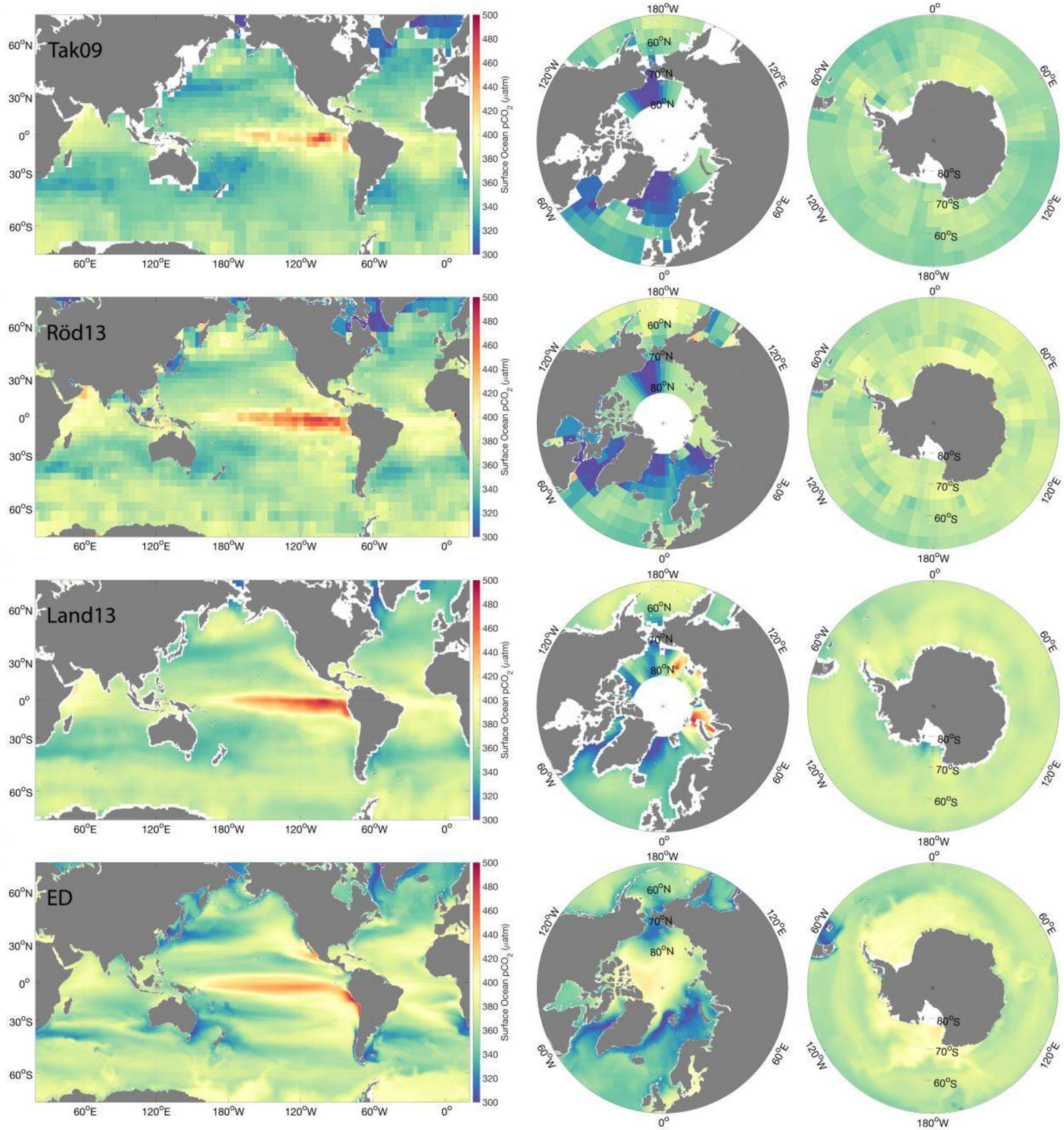

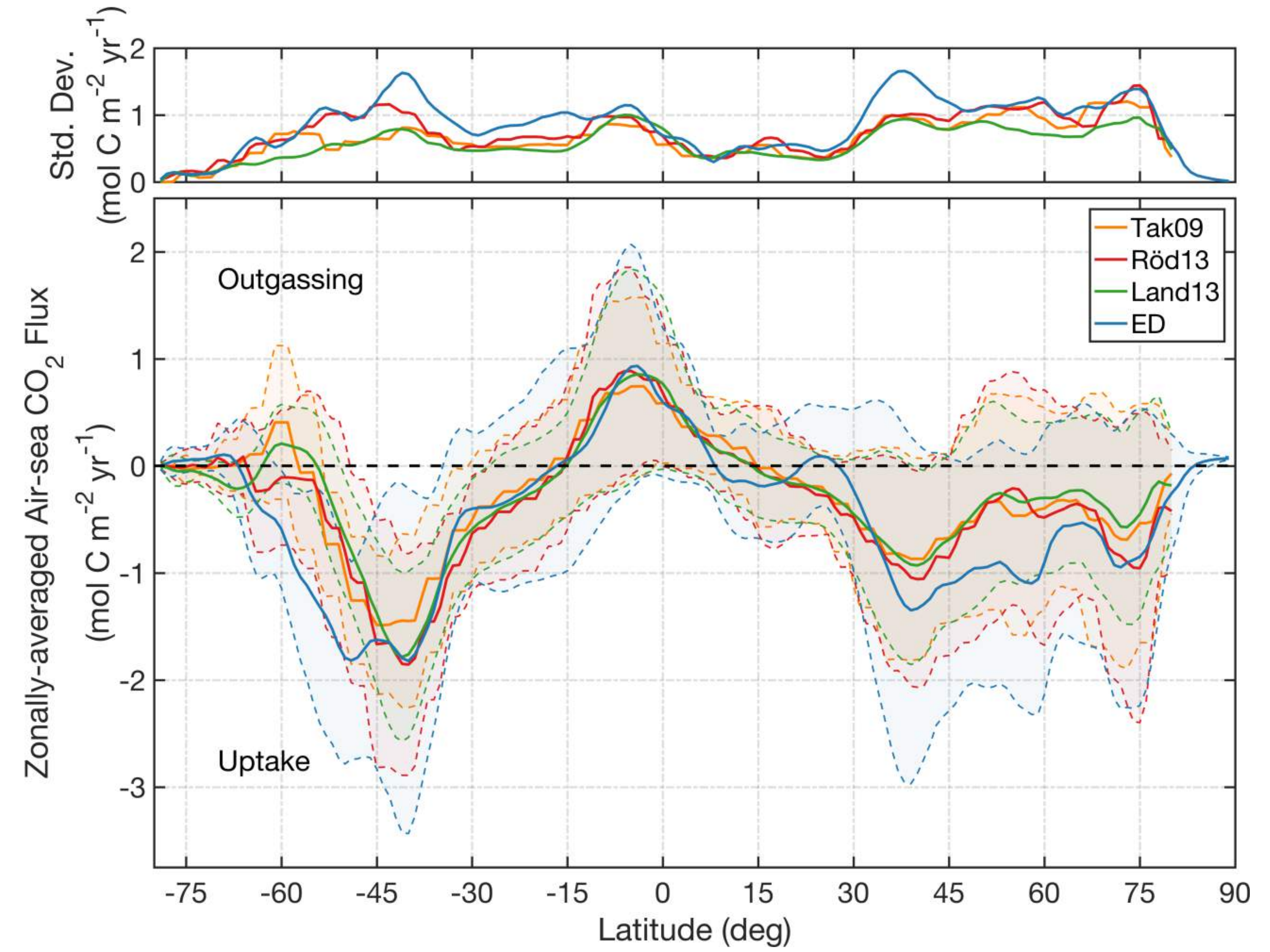

Std. Dev.
(mol C m-2 yr-1)
2
1
0
Tak09
Röd13
Land13
ED
Outgassing
Uptake
Zonally-averaged Air-sea CO2 Flux
(mol C m-2 yr-1)
2
1
0
-1
-2
-3
-75
-60
-45
-30
-15
0
15
30
45
60
75
90
Latitude (deg)

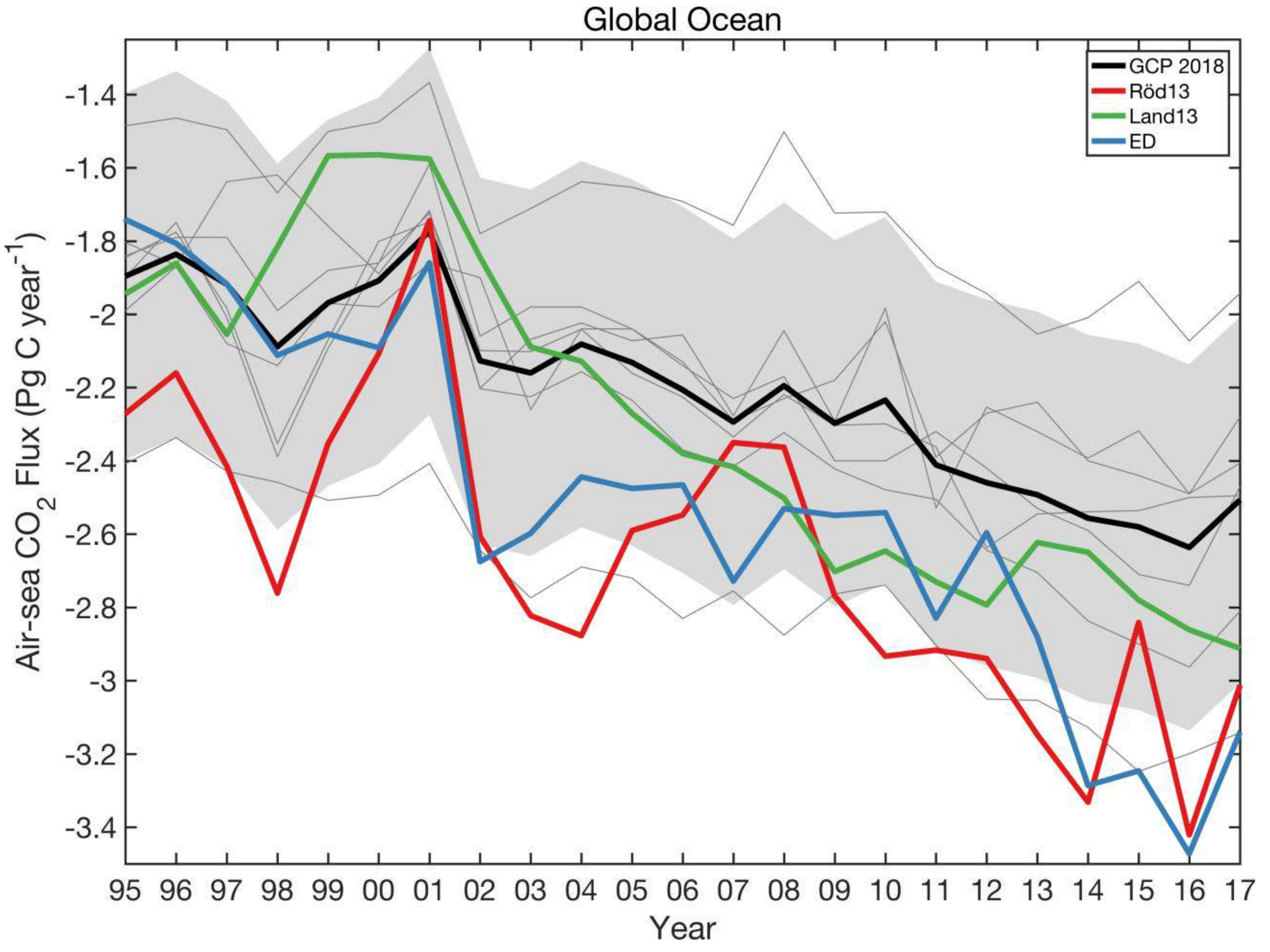

Global Ocean
GCP 2018
Röd13
Land13
ED
Air-sea CO_2 Flux (Pg C year^{-1})
-1.4
-1.6
-1.8
-2
-2.2
-2.4
-2.6
-2.8
-3
-3.2
-3.4
95
96
97
98
99
00
01
02
03
04
05
06
07
08
09
10
11
12
13
14
15
16
17
Year

Fay and McKinley (2014) biomes used to compute area-weighted mean surface ocean pCO_2 and spatially-integrated air-sea CO_2 fluxes.

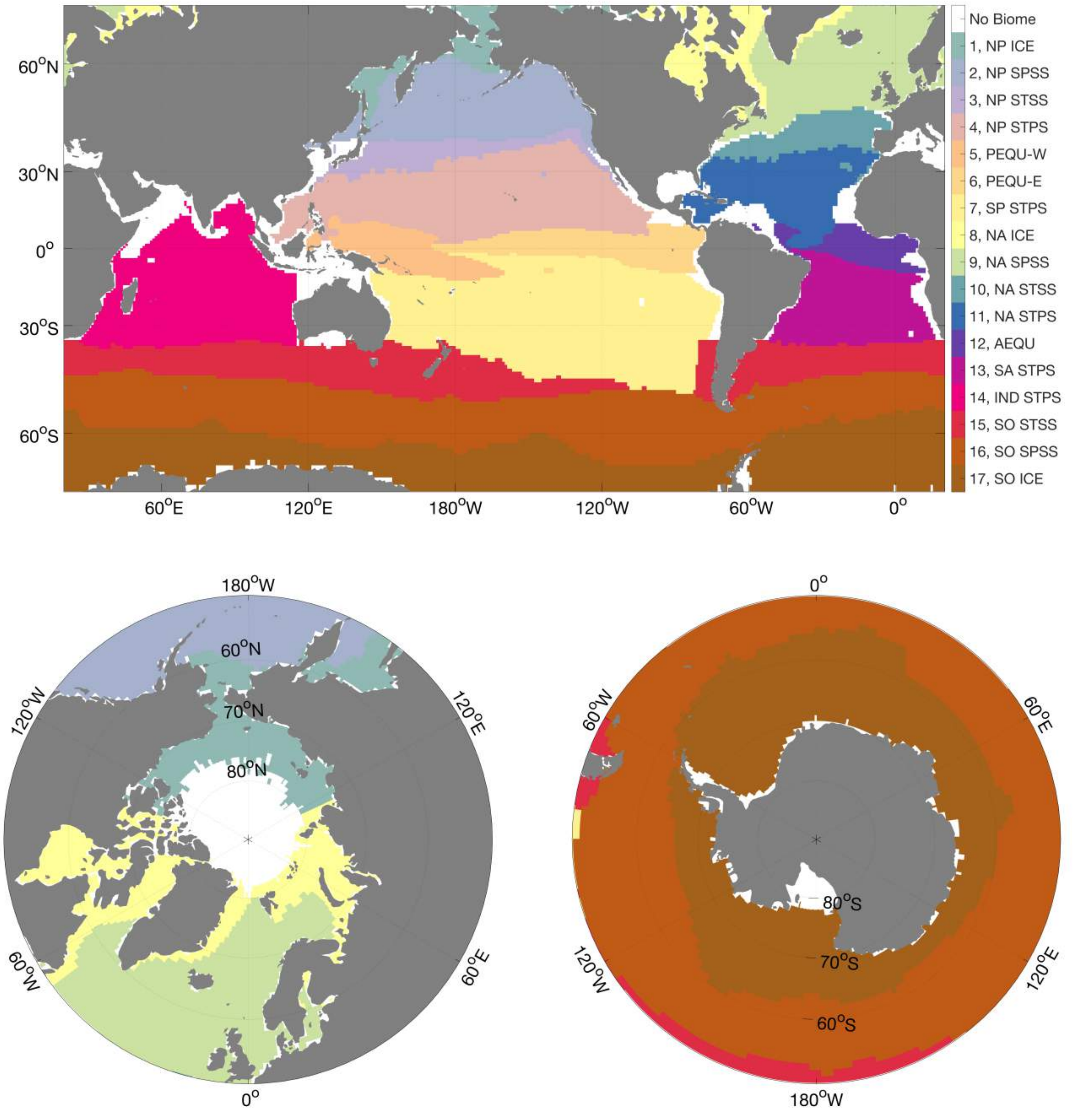

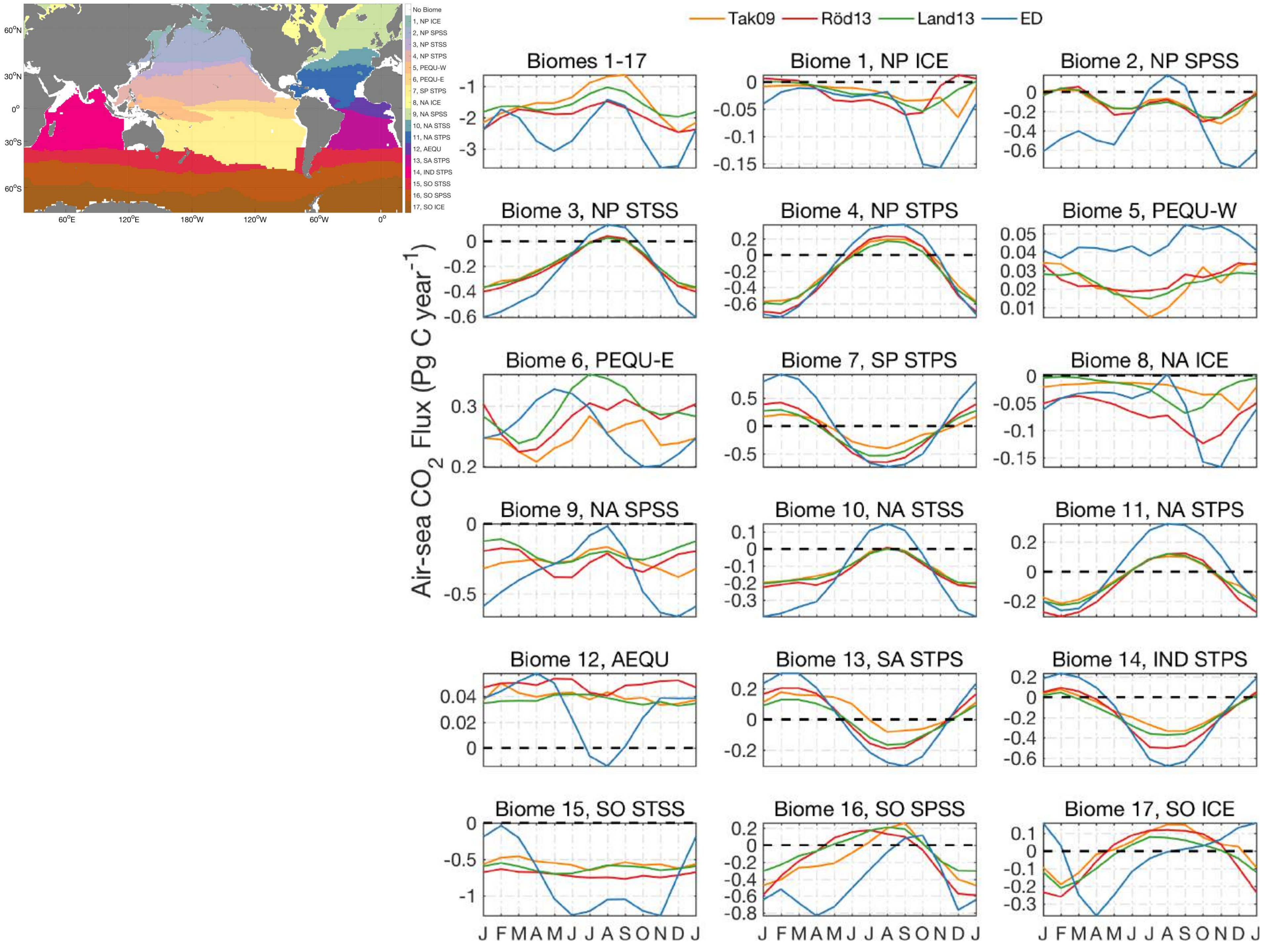

No Biome
1, NP ICE
2, NP SPSS
3, NP STSS
4, NP STPS
5, PEQU-W
6, PEQU-E
7, SP STPS
8, NA ICE
9, NA SPSS
10, NA STSS
11, NA STPS
12, AEQU
13, SA STPS
14, IND STPS
15, SO STSS
16, SO SPSS
17, SO ICE
Tak09
Röd13
Land13
ED
Biomes 1-17
Biome 1, NP ICE
Biome 2, NP SPSS
Biome 3, NP STSS
Biome 4, NP STPS
Biome 5, PEQU-W
Biome 6, PEQU-E
Biome 7, SP STPS
Biome 8, NA ICE
Biome 9, NA SPSS
Biome 10, NA STSS
Biome 11, NA STPS
Biome 12, AEQU
Biome 13, SA STPS
Biome 14, IND STPS
Biome 15, SO STSS
Biome 16, SO SPSS
Biome 17, SO ICE
Air-sea CO_2 Flux (Pg C $year^{-1}$)
J F M A M J J A S O N D J

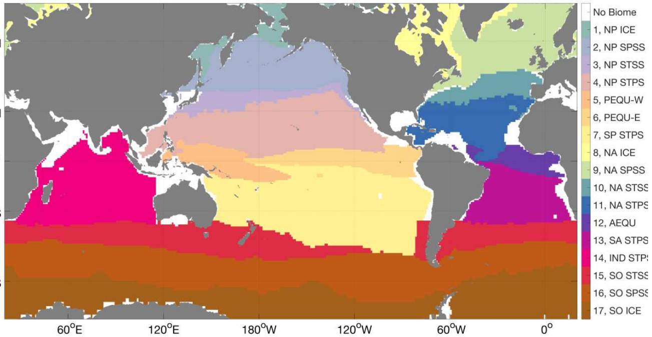

No Biome
1, NP ICE
2, NP SPSS
3, NP STSS
4, NP STPS
5, PEQU-W
6, PEQU-E
7, SP STPS
8, NA ICE
9, NA SPSS
10, NA STSS
11, NA STPS
12, AEQU
13, SA STPS
14, IND STPS
15, SO STSS
16, SO SPSS
17, SO ICE
60°N
30°N
0°
30°S
60°S
60°E
120°E
180°W
120°W
60°W
0°

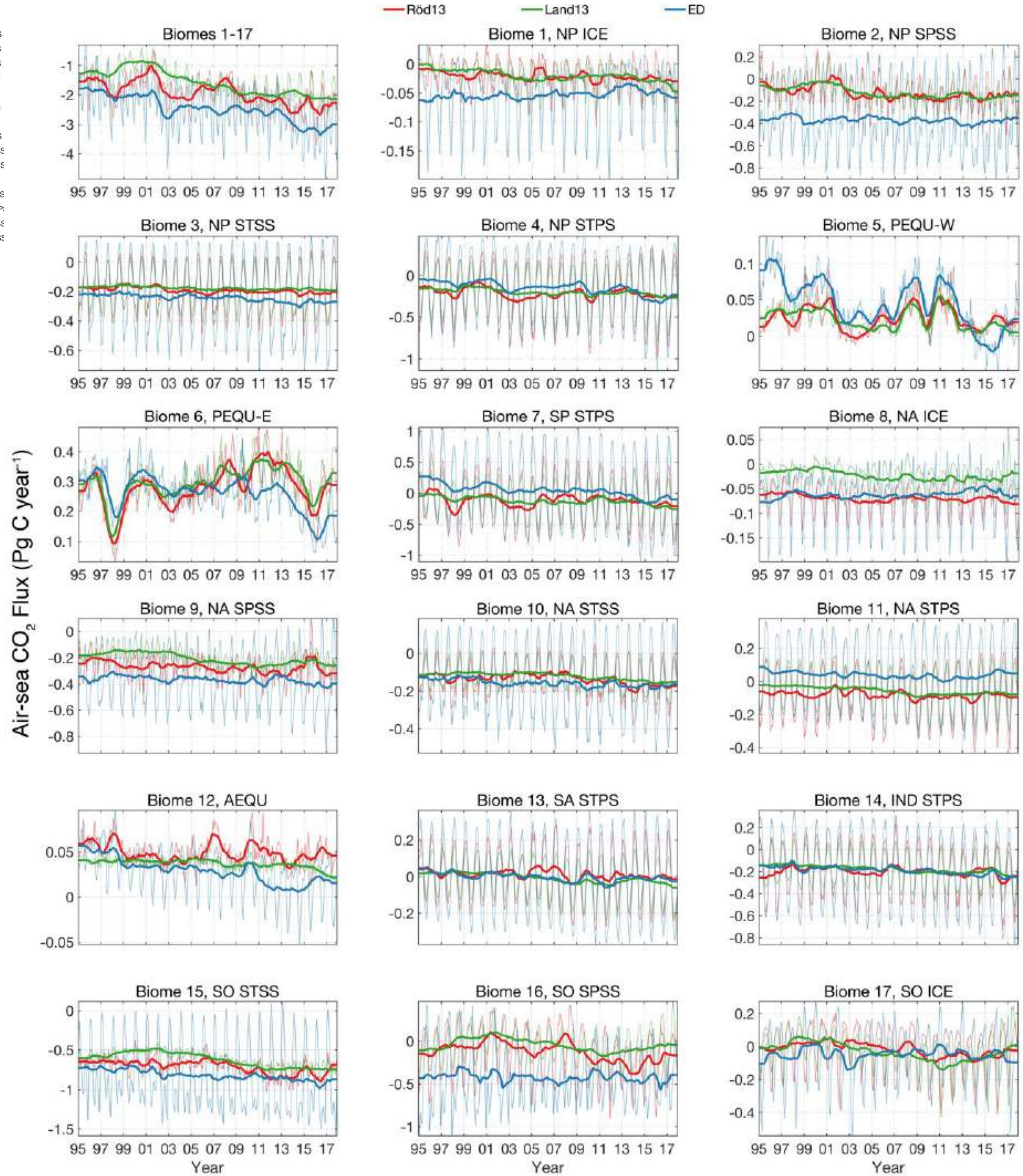

Röd13
Land13
ED
Biomes 1-17
Biome 1, NP ICE
Biome 2, NP SPSS
Biome 3, NP STSS
Biome 4, NP STPS
Biome 5, PEQU-W
Biome 6, PEQU-E
Biome 7, SP STPS
Biome 8, NA ICE
Biome 9, NA SPSS
Biome 10, NA STSS
Biome 11, NA STPS
Biome 12, AEQU
Biome 13, SA STPS
Biome 14, IND STPS
Biome 15, SO STSS
Biome 16, SO SPSS
Biome 17, SO ICE
Air-sea CO2 Flux (Pg C year-1)
95 97 99 01 03 05 07 09 11 13 15 17
Year

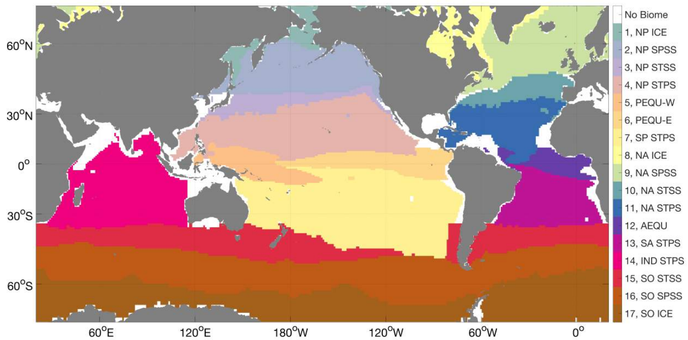

Monthly time series of surface ocean fCO_2 for Surface Ocean CO_2 Atlas (SOCAT) v5 (black) and corresponding ECCO-Darwin v4 (red) taken at same time-space locations.

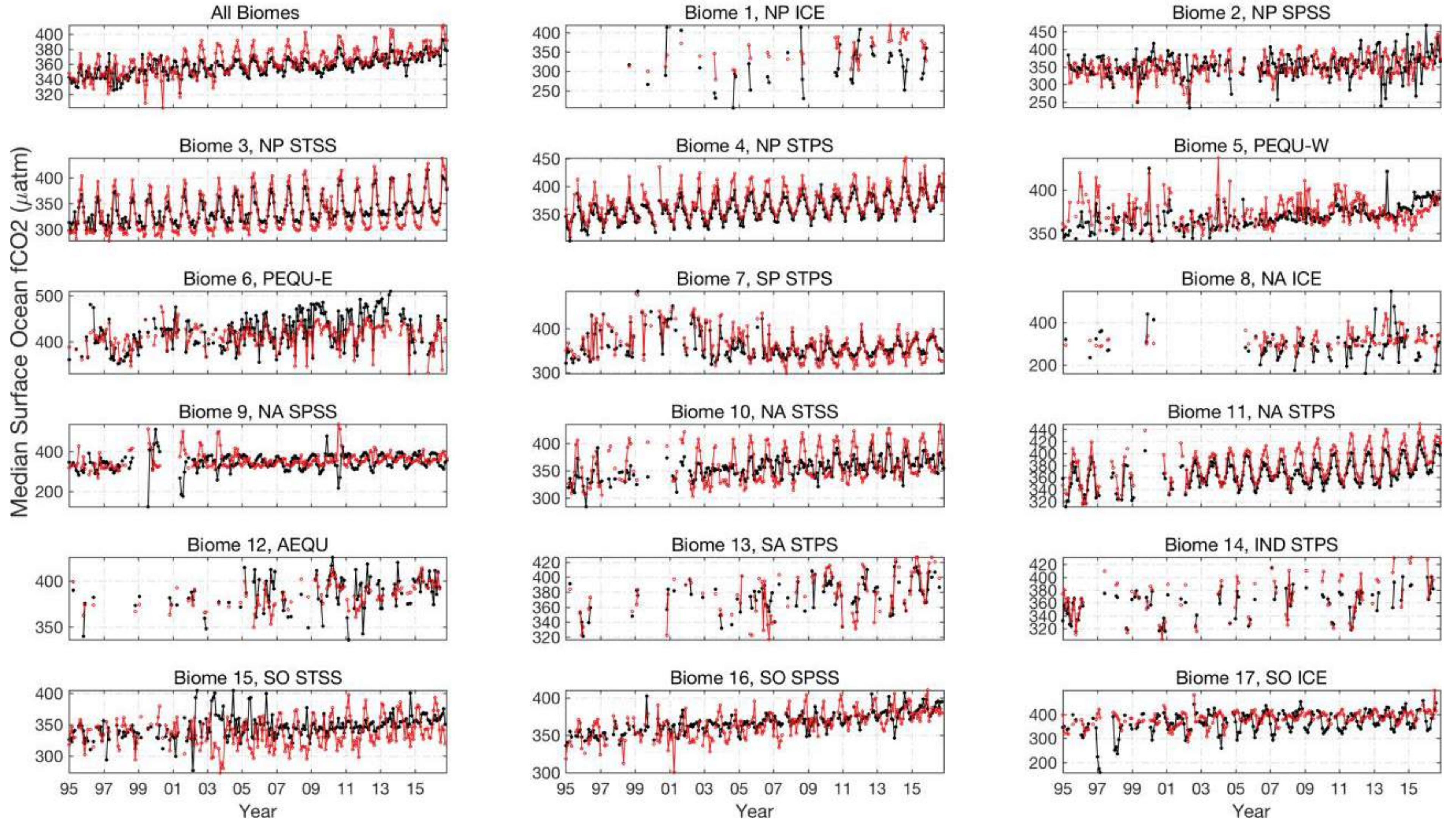

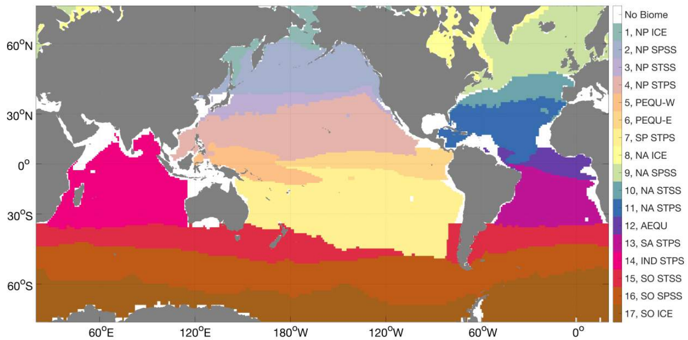

Number of observation-model surface ocean *f*CO_2 points per month for each biome.

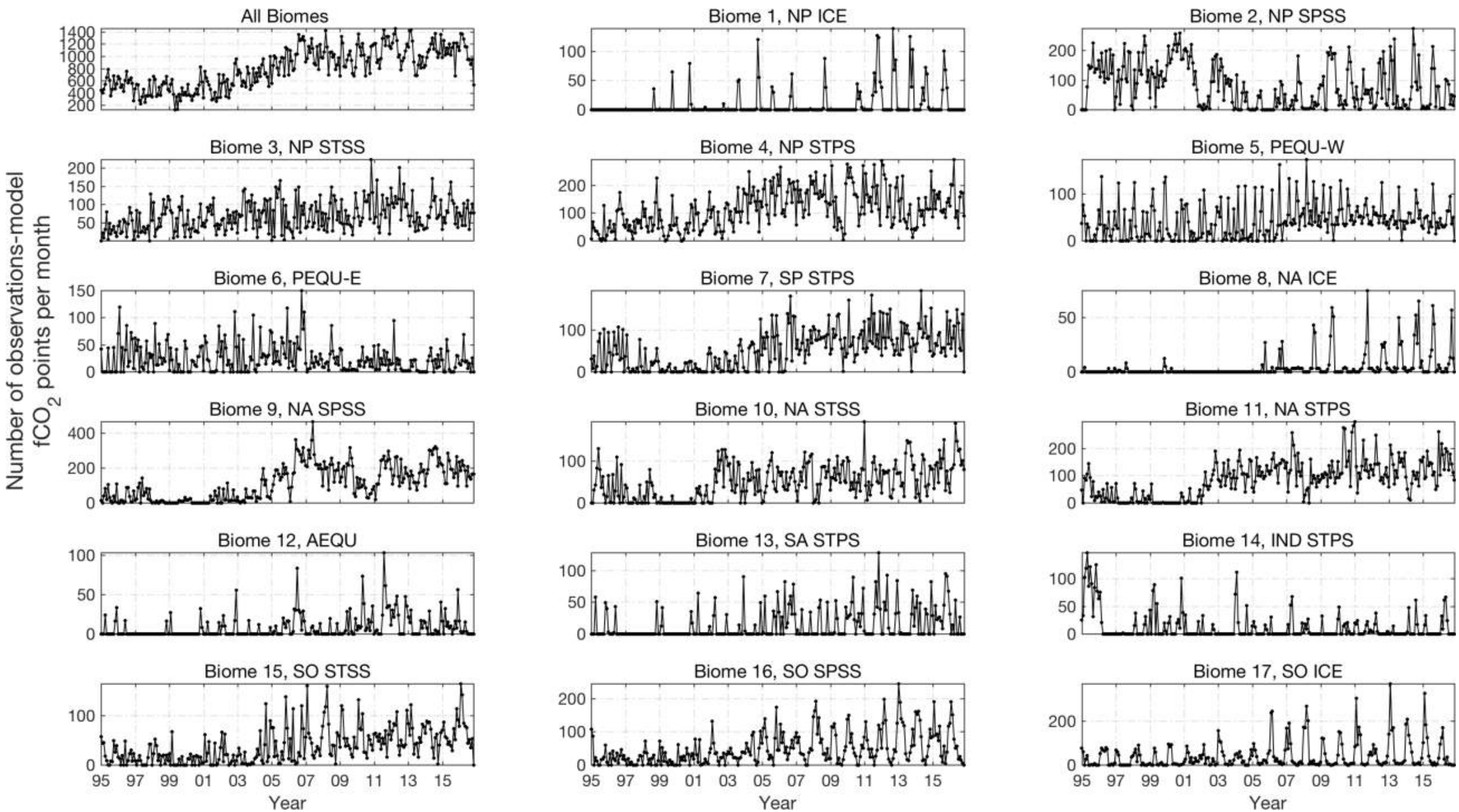

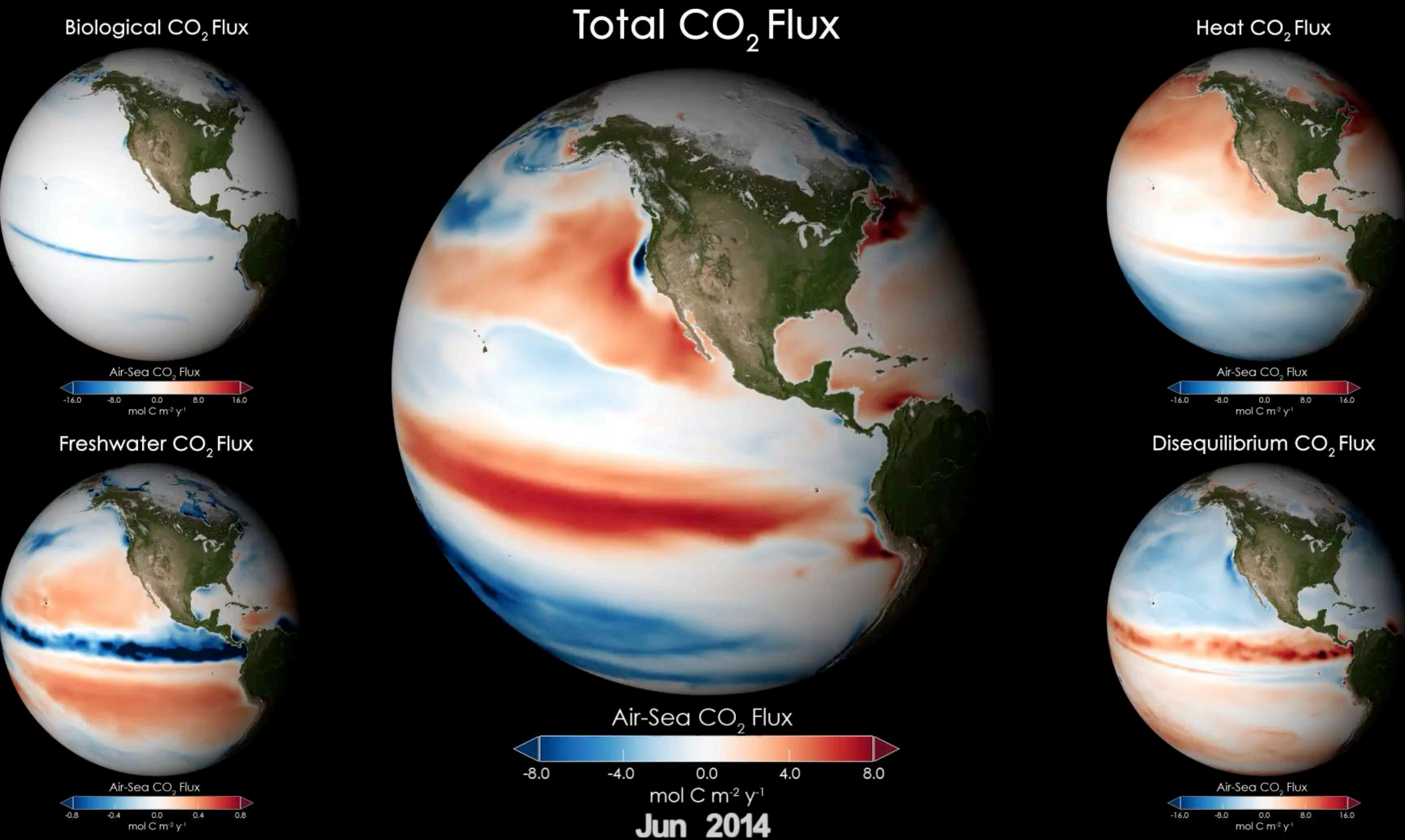

Biological CO_2 Flux
Total CO_2 Flux
Heat CO_2 Flux
Air-Sea CO_2 Flux
-16.0 -8.0 0.0 8.0 16.0
mol C m^{-2} y^{-1}
Air-Sea CO_2 Flux
-16.0 -8.0 0.0 8.0 16.0
mol C m^{-2} y^{-1}
Freshwater CO_2 Flux
Disequilibrium CO_2 Flux
Air-Sea CO_2 Flux
-8.0 -4.0 0.0 4.0 8.0
mol C m^{-2} y^{-1}
Jun 2014
Air-Sea CO_2 Flux
-0.8 -0.4 0.0 0.4 0.8
mol C m^{-2} y^{-1}
Air-Sea CO_2 Flux
-16.0 -8.0 0.0 8.0 16.0
mol C m^{-2} y^{-1}

Summary and concluding remarks

- ECCO-Darwin v4 produces air-sea CO2 fluxes that exhibit broad-scale consistency with interpolation-based products, particularly in the subtropical and equatorial biomes.

- The largest differences between estimates in long-term ocean CO_2 uptake occur in subpolar seasonally-stratified biomes, where ECCO-Darwin produces stronger winter uptake.

- Compared to the Global Carbon Project (GCP) ocean biogeochemistry models, ECCO-Darwin has global CO_2 sink (time-mean of -2.52 ± 0.49 Pg C $year^{-1}$) and interannual variability that is more consistent with the interpolation-based products.

- Contrary to interpolation-based products, ECCO-Darwin is less sensitive to sparse and uneven observational sampling and it permits full attribution of the inferred air-sea CO_2 flux spatiotemporal variability.

ECCO-Darwin v4 model output on NAS portal
https://data.nas.nasa.gov

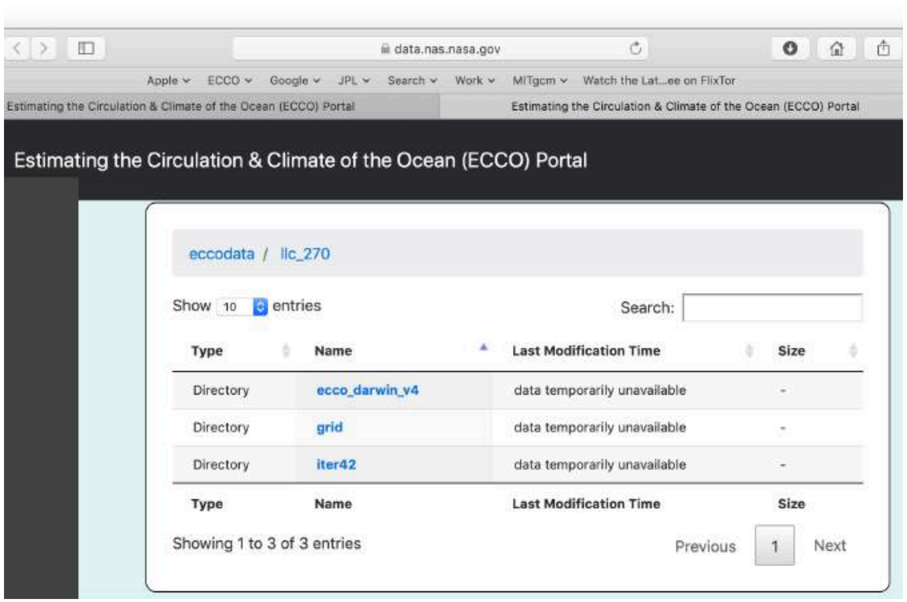

Instructions for rerunning on MITgcm CVS server:
http://wwwcvs.mitgcm.org/viewvc/MITgcm/

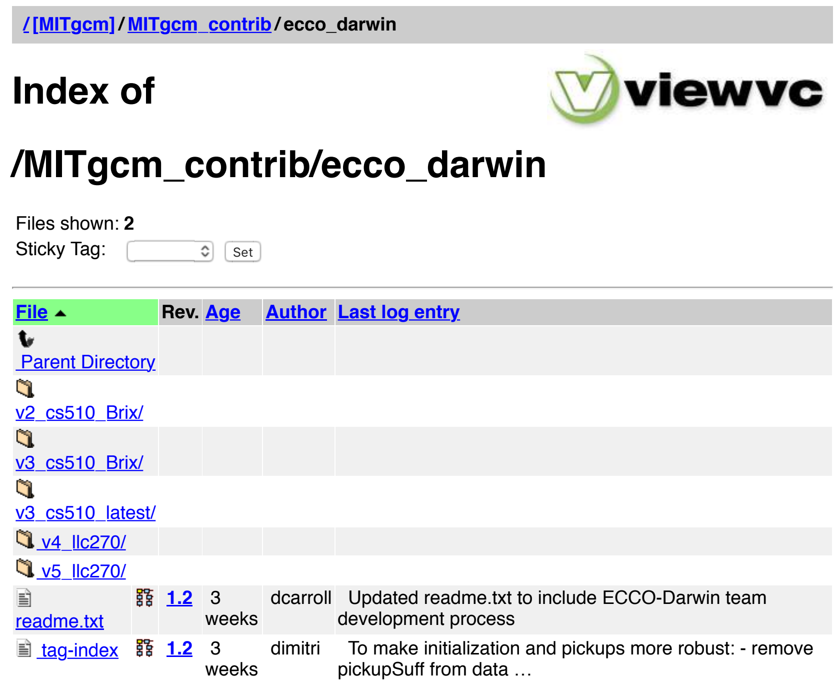

Preprint available @ https://tinyurl.com/y5p539s6

Surrender? We have not yet begun to fight!